

# Trends of Extreme Precipitation in Eastern China and Their Possible Causes

LIU Run<sup>1</sup>, LIU Shaw Chen<sup>\*2,3</sup>, Ralph J. CICERONE<sup>4,5</sup>, SHIU Chein-Jung<sup>2</sup>,  
LI Jun<sup>1</sup>, WANG Jingli<sup>6</sup>, and ZHANG Yuanhang<sup>\*1</sup>

<sup>1</sup>State Key Joint Laboratory of Environmental Simulation and Pollution Control,  
College of Environmental Sciences and Engineering, Peking University, Beijing 100871

<sup>2</sup>Research Center for Environmental Changes, Academia Sinica, Taipei 11529

<sup>3</sup>Department of Atmospheric Science, NCU, Zhongli 32001

<sup>4</sup>National Academy of Sciences, Washington DC 20001, USA

<sup>5</sup>Earth System Science, University of California, Irvine 92697-3100, USA

<sup>6</sup>Institute of Urban Meteorology of China Meteorological Administration, Beijing 100089

(Received 2 January 2015; revised 9 March 2015; accepted 27 March 2015)

## ABSTRACT

Significant increases of heavy precipitation and decreases of light precipitation have been reported over widespread regions of the globe. Global warming and effects of anthropogenic aerosols have both been proposed as possible causes of these changes. We examine data from urban and rural meteorological stations in eastern China (1955–2011) and compare them with Global Precipitation Climatology Project (GPCP) data (1979–2007) and reanalysis data in various latitude zones to study changes in precipitation extremes. Significant decreases in light precipitation and increases in heavy precipitation are found at both rural and urban stations, as well as low latitudes over the ocean, while total precipitation shows little change. Characteristics of these changes and changes in the equatorial zone and other latitudes suggest that global warming rather than aerosol effects is the primary cause of the changes. In eastern China, increases of annual total dry days (28 days) and  $\geq 10$  consecutive dry days (36%) are due to the decrease in light precipitation days, thereby establishing a causal link among global warming, changes in precipitation extremes, and higher meteorological risk of floods and droughts. Further, results derived from the GPCP data and reanalysis data suggest that the causal link exists over widespread regions of the globe.

**Key words:** extreme precipitation, global warming, aerosols, meteorological risk of floods and droughts

**Citation:** Liu, R., S. C. Liu, R. J. Cicerone, C.-J. Shiu, J. Li, J. L. Wang, and Y. H. Zhang, 2015: Trends of extreme precipitation in eastern China and their possible causes. *Adv. Atmos. Sci.*, **32**(8), 1027–1037, doi: 10.1007/s00376-015-5002-1.

## 1. Introduction

Significant increases of heavy precipitation, sometimes with decreases of light and moderate precipitation, have been reported over extensive land areas (e.g. Karl and Knight, 1998; Manton et al., 2001; Klein Tank and Können, 2003; Fujibe et al., 2005; Groisman et al., 2005; Goswami et al., 2006; Qian et al., 2010; Benestad, 2013). Specifically for China, similar changes have been reported in a large number of studies (e.g. Liu et al., 2005; Qian et al., 2007; Wang and Zhai, 2008; Zhu et al., 2009; Wu and Fu, 2013; Jiang et al., 2014). In fact, increases of heavy precipitation and decreases of light and moderate precipitation have been found at most latitudes within 60°S–60°N (Liu et al., 2009; Shiu et al., 2012), even over tropical oceans (Lau and Wu, 2007,

2011). Overall, there have been increases of precipitation intensity as a result of the combination of increases in heavy precipitation and decreases in light precipitation, i.e. there is a shift from light precipitation toward heavy precipitation.

It is known that global warming can enhance precipitation intensity and thus change precipitation extremes (Trenberth, 1998; Allen and Ingram, 2002; Semenov and Bengtsson, 2002; Trenberth et al., 2003). Increases in heavy precipitation can increase surface runoff and lead to more and worse floods and mudslides; while decreases of light and moderate precipitation can lengthen dry spells and increase the meteorological risk of drought because light and moderate precipitation is a critical source of soil moisture as well as ground water. Nevertheless, attributing increases of floods and/or droughts to global warming has been problematic for a number of reasons. First, quantifying trends of floods and droughts is difficult because there is no well-established index for floods and droughts, particularly in terms of their degrees of severity. Second, extensive flood-control and drought-prevention en-

\* Corresponding authors:

LIU Shaw Chen, shawliu@gate.sinica.edu.tw

ZHANG Yuanhang, yzhzhang@pku.edu.cn

gineering such as dams and irrigation systems can drastically change observed trends of floods and droughts. In addition, short-term aerosol effects have also been proposed to change the precipitation intensity and thus the extremes (Warner and Twomey, 1967; Gong et al., 2007). Here, we differentiate short-term aerosol effects, which include microphysical and radiative effects of aerosols with a time scale up to several days, from the long-term effect of aerosols on the climate, which is part of global warming with a time scale of decades.

The quantity of global total annual precipitation, which is equal to global evaporation and determined by the global surface energy budget, increases with global temperature at a rather small rate of about 2%–3%  $K^{-1}$  (Cubasch et al., 2001). Analysis during the Intergovernmental Panel on Climate Change's Fourth Assessment Report (AR4) of two long-term gauge-based precipitation datasets over land—the Global Historical Climatology Network (GHCN) (Vose et al., 1992) and Climatic Research Unit (Mitchell and Jones, 2005) datasets—showed that the annual average total precipitation of both datasets possessed small linear increasing trends, but that they were not statistically significant (Trenberth et al., 2007). Other periods covered in AR4 (1951–2005 and 1979–2005) show a mix of negative and positive trends, depending on the dataset. These small and/or lack of clear trends in the annual total precipitation are consistent with the predicted small increase in global precipitation/evaporation with global warming. Therefore, this study will focus on the increase in the precipitation intensity and associated changes in precipitation extremes, rather than the total precipitation.

Trenberth et al. (2003) summarized the global warming hypothesis by explaining that the precipitation intensity of storms should increase at about the same rate as atmospheric moisture, which is about 7%  $K^{-1}$  according to the Clausius–Clapeyron equation. They further argued that the increase in heavy rainfall could even exceed 7%  $K^{-1}$  because additional latent heat released from the increased water vapor could invigorate the storms. An invigorated storm could remove moisture at a rate of more than 7%  $K^{-1}$  from the atmosphere. Meanwhile, as mentioned earlier, global evaporation would increase by about 2%–3%  $K^{-1}$  only, leaving less moisture for light and moderate precipitation. Moreover, the increase of latent heat in the upper troposphere from storms can reduce the lapse rate. The lapse rate is also reduced as a result of a robust water vapor–lapse rate climate feedback effect in coupled ocean–atmosphere models (Held and Soden, 2006). The reduced lapse rate makes the atmosphere more stable and thus less likely to precipitate, especially for light and moderate precipitation that requires an unstable large-scale environment. The combined effect is to increase the precipitation intensity by enhancing heavy precipitation while suppressing light and moderate precipitation. These thermodynamic arguments were broadly confirmed by an analysis of model-simulated changes by Sun et al. (2007) and analyses of observational data by Liu et al. (2009) and Shiu et al. (2012), who examined observed precipitation from the Global Precipitation Climatology Project (GPCP) and reanalysis.

It has been long recognized that aerosols may have a significant influence on clouds and precipitation by acting as cloud condensation nuclei (Warner and Twomey, 1967; Albrecht, 1989; Ramanathan et al., 2001; Andreae et al., 2004; Dai et al., 2008; Koren et al., 2008). The aerosol effect on precipitation processes, considered part of the “Albrecht” effect—the “second indirect” effect on cloud extent and life time (Ackerman et al., 1978; Albrecht, 1989; Hansen et al., 1997)—is complex and uncertain, especially for mixed-phase convective clouds (Tao et al., 2012). There have been numerous studies conducted on the effects of aerosol on total precipitation over different periods (e.g. annual, seasonal), producing mixed results. An excellent example is Warner (1971), who concluded there was no change in 60 years of precipitation due to aerosols emitted from sugarcane burning in northern Australia. In addition, a report by the U.S. National Research Council (2003) concluded “there still is no convincing scientific proof of the efficacy of international weather modification efforts,” of which many are modification efforts using aerosols.

A number of recent studies suggest that aerosols can invigorate large convections by suppressing the onset of precipitation, pulling in more moisture, releasing more latent heat, pushing moisture to higher altitude and forming more ice clouds; while for small, low clouds the action stops at suppressing the onset of precipitation and burning off the clouds (Andreae et al., 2004; Lin et al., 2006; Jiang et al., 2008; Koren et al., 2008; Rosenfeld et al., 2008; Tao et al., 2012). The net effect is to suppress light precipitation and enhance heavy precipitation. Nevertheless, there remain large uncertainties concerning the effect of aerosols on precipitation and its intensity (Levin and Cotton, 2009; Yang et al., 2011a; Boucher et al., 2013).

## 2. Approach and data

We first examine GPCP precipitation data (V1.0, 1979–2007,  $2.5^\circ \times 2.5^\circ$ , pentad) (Xie et al., 2003) over the oceanic region between  $10^\circ S$  and  $10^\circ N$  and analyze the relationship between changes in precipitation extremes and SST anomalies. This region is remote to, and free from, the influence of anthropogenic emissions. Significant changes in the precipitation intensity and associated extreme precipitation in this oceanic region are expected to be more likely driven by global warming, rather than the short-term aerosol effect. Results of the  $10^\circ S$ – $10^\circ N$  oceanic region are then compared to those at higher latitudes in the Northern Hemisphere ( $10^\circ$ – $20^\circ N$ , and the  $20^\circ$ – $45^\circ N$  land area) and eastern China, where there are more aerosols to evaluate the cause of changes in the precipitation intensity and associated extreme precipitation. The choice of the  $20^\circ$ – $45^\circ N$  land area is intended to overlap with eastern China, to facilitate comparison.

Daily precipitation data observed at 101 out of a total 194 international exchange meteorological stations operated by the China Meteorological Administration during the period 1955–2011 are also used in this study (<http://cdc.cma.gov.cn/>)

home.do). The 101 stations, which cover about 40% of total area and represent important agricultural regions of China, are chosen for their relatively high annual average precipitation of over 500 mm and for their completeness of data (<5 missing days annually). Stations with precipitation of less than 500 mm yr<sup>-1</sup> (mostly in semi-arid northwestern China) are excluded because their interannual variations are too large to derive any statistically meaningful trends.

During the period 1955–2011, the consumption in China of fossil fuel, and thus emissions of aerosols, increased by a factor of about 15 (Streets et al., 2000; Lu et al., 2010; National Bureau of Statistics of China, 2012). Satellite images clearly show the extremely high values and large increasing trends of aerosol optical depth over industrialized areas in China. Given these large temporal and spatial ranges in the concentration of aerosols, if aerosols can significantly affect the precipitation intensity, one would expect to detect significant differences among the trends of different regions, as well as an urban–rural difference in the trend. Figure 1 shows the distribution of the 101 stations. It can be seen that most of the stations selected are located in eastern China, which is influenced strongly by the East Asian Monsoon, with moisture mainly from the western Pacific and, to a lesser degree, Indian Ocean. The 101 stations are classified into 45 urban and 56 rural stations according to their land-use data from the Moderate Resolution Imaging Spectroradiometer ([https://lpdaac.usgs.gov/products/modis\\_products\\_table](https://lpdaac.usgs.gov/products/modis_products_table)). This classification is substantiated by the temperature difference between urban and rural stations, which shows a clear urban heat island effect (Yang et al., 2011b; Wang and Ge, 2012).

Surface air temperature is taken from GHCN-Monthly,

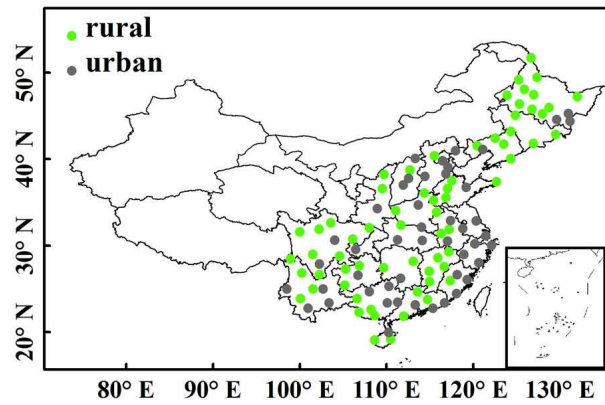


**Fig. 1.** Geographical distributions of the 101 surface international exchange meteorological stations in eastern China with average annual precipitation over 500 mm. Gray dots denote 45 urban stations, light green 56 rural stations.

version 3.2.1 (Peterson and Vose, 1997; Jones and Moberg, 2003). SST is taken from the Extended Reconstructed Sea Surface Temperature dataset, v3b (Xue et al., 2003; Smith et al., 2008).

### 3. Changes of precipitation intensity over the equatorial oceanic area

Using the GPCP pentad data (1979–2007), we find significant trends in the top 30% heavy precipitation and bottom 30% light precipitation in the equatorial oceanic region between 10°S and 10°N (Fig. 2a). The values shown are annual

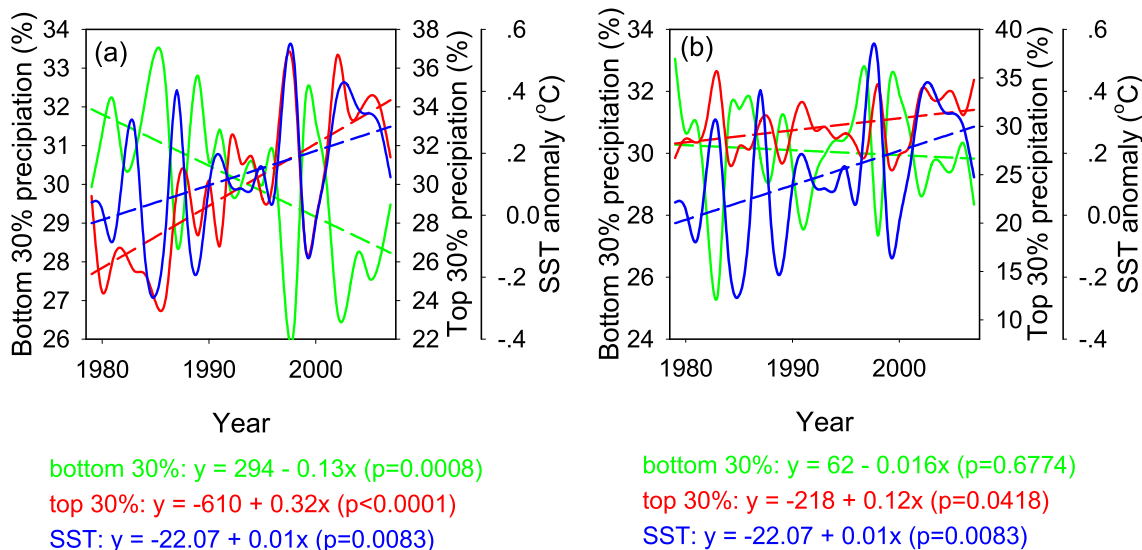


**Fig. 2.** (a) Temporal variations of annual average amounts of precipitation (units: %) in two intensity bins for the oceanic region between 10°S and 10°N from GPCP pentad data: bottom 30% light precipitation (green, left coordinate) and top 30% heavy precipitation (red, right coordinate); and the SST anomaly between 10°S and 10°N (blue, right offset coordinate). Dashed lines are linear regressions. (b) As in (a) but from ECMWF ERA-Interim reanalysis data (1979–2007).

average amounts of precipitation (units: %) falling within the specified catalog for all oceanic grids between  $10^{\circ}\text{S}$  and  $10^{\circ}\text{N}$ . There are a total of 81 322 pentad data points in each year in this oceanic zone, sufficiently large for subset statistical analyses. Linear trends of the top 30% of heavy precipitation and the bottom 30% light precipitation are  $3.2\%$  ( $10\text{ yr}^{-1}$ ) and  $-1.3\%$  ( $10\text{ yr}^{-1}$ ), respectively, both significant at the 95% confidence level. In combination, these trends imply a significant increase in the precipitation intensity. Also plotted in Fig. 2a is the SST in this region. There is an obvious anti-correlation between the bottom 30% light precipitation and SST, with a correlation coefficient of  $R = -0.74$ . These correlations and trends are in good agreement with the global warming hypothesis summarized by Trenberth et al. (2003). Since there are negligible anthropogenic emissions in this region, it is reasonable to propose that the increase in SST is the primary cause of the increase in heavy precipitation and the decrease in light precipitation, and their combined increase in precipitation intensity in the equatorial ocean region.

Another piece of evidence in support of the increase in SST being the primary cause of the increase in heavy precipitation and the decrease in light precipitation in the equatorial ocean region is shown in Fig. 2b, in which the bottom 30% light precipitation and top 30% heavy precipitation from European Centre for Medium-Range Weather Forecasts Interim Reanalysis (ERA-Interim) data are plotted together with the SST in the equatorial oceanic region between  $10^{\circ}\text{S}$  and  $10^{\circ}\text{N}$ . Precipitation reanalysis products from operational weather forecast models that do not use observed precipitation instead calculate precipitation from observed moisture and winds, thus providing independent information as compared to the GPCP data. The general patterns in Fig. 2b are practically the same as those in Fig. 2a, e.g. good anti-correlation between the top 30% and bottom 30% precipitation ( $R = -0.86$ ) and good correlation between SST and the top 30% precipitation ( $R = 0.71$ ). The weather forecast model used in the reanalysis included the thermodynamic processes described in Trenberth et al. (2003), but did not include the aerosol effects. For instance, observed vertical water vapor column abundance in the reanalysis model increased by  $7\%$   $\text{K}^{-1}$ , consistent with the prediction of the Clausius–Clapeyron equation (Trenberth et al., 2003), and the reanalysis model included the increased latent heat and subsequent invigoration of the storm due to the increase in water vapor. On the other hand, since it is very unlikely that anthropogenic aerosols could significantly affect the moisture and winds over the remote equatorial oceanic region, we propose that the large increase in the top 30% heavy precipitation and the significant anti-correlation between the top 30% heavy precipitation and the bottom 30% light precipitation obtained by the ERA-Interim reanalysis model are very likely driven primarily by the thermodynamic processes rather than the short-term anthropogenic aerosol effects. Thus, we can conclude that, at least on a yearly basis, the increase in SST (which is part of global warming) rather than anthropogenic aerosols is likely the primary driving force for the increase in precipitation intensity observed over the equatorial oceans

shown in the GPCP data during 1979–2007.

#### 4. Changes of precipitation intensity at higher latitudes

In Fig. 3 the changes in precipitation intensity in the equatorial oceanic region over  $10^{\circ}\text{S}$ – $10^{\circ}\text{N}$  are compared to those of higher latitudes in the Northern Hemisphere; specifically, the  $10^{\circ}$ – $20^{\circ}\text{N}$  zone and land areas in the  $20^{\circ}$ – $45^{\circ}\text{N}$  zone. Values in Fig. 3 are evaluated using an interannual difference method developed by Liu et al. (2009). The interannual difference method is an effective tool to study the relationship between two parameters that both change with time. In this case, the two parameters are precipitation and surface temperature. Briefly, for the case of the  $10^{\circ}\text{S}$ – $10^{\circ}\text{N}$  oceanic region, all precipitation data in the entire period of 1979–2007 are gathered together and sorted into 10 bins of equal precipitation amount in increasing precipitation intensity. Ranges of the 10 bins are determined by this sorting and fixed throughout the analysis. The precipitation amount within each bin for a given year is sorted in the same way with the fixed ranges. The  $\Delta P$  of each bin in Fig. 3 is the difference in the precipitation amount for each bin between any two years within 1979–2007, including pairs not adjacent to each other, such as 1999 and 2007, and the  $\Delta T$  is the corresponding difference in the observed surface air temperature of  $30^{\circ}\text{S}$ – $30^{\circ}\text{N}$ . The

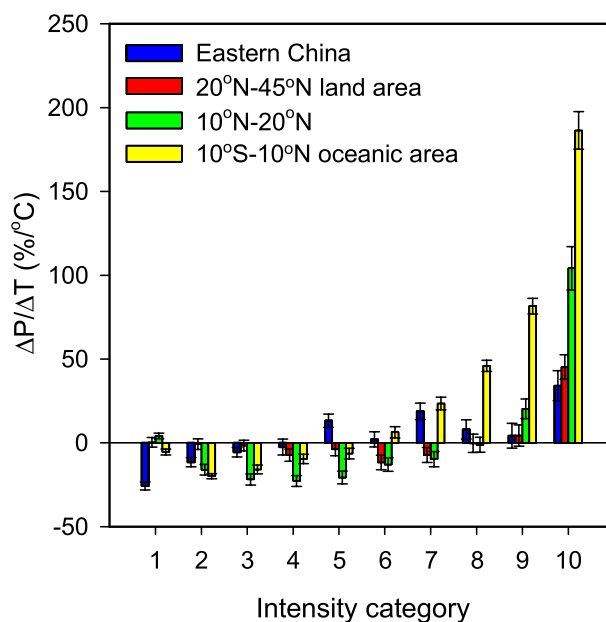


**Fig. 3.** Changes in the annual precipitation amount falling within each of the ten intensity bins ( $\Delta P$ ) for a  $1^{\circ}$  increase in annual average temperature in the  $30^{\circ}\text{S}$ – $30^{\circ}\text{N}$  zone ( $\Delta T$ ). Blue bars denote  $\Delta P/\Delta T$  values derived from data of all 101 stations in eastern China in 1979–2007. Yellow, green and red bars are  $\Delta P/\Delta T$  values derived for the  $10^{\circ}\text{S}$ – $10^{\circ}\text{N}$  oceanic area,  $10^{\circ}$ – $20^{\circ}\text{N}$  zone and  $20^{\circ}$ – $45^{\circ}\text{N}$  land area from GPCP pentad data (1979–2007), respectively. The vertical line on top of each bar denotes the standard error of the mean.

values ( $\Delta P/\Delta T$ ) shown in Fig. 3 are the slopes between  $\Delta P$  and  $\Delta T$ , which represent the change in the annual precipitation amount falling within each of the ten intensity bins ( $\Delta P$ ), for one degree Kelvin increase in annual average temperature of 30°S–30°N ( $\Delta T$ ).

We have compared results obtained by the interannual difference method to those of a direct scatter plot between the precipitation and temperature, and to those calculated from individual linear trends of the precipitation and temperature. Agreement within standard errors of the mean (SEM) of the three methods is found for all cases shown in Fig. 3, and the interannual difference method renders the lowest value for SEM.

The temperature of 30°S–30°N is used for all four regions in Fig. 3 for ease of comparison. According to the thermodynamic hypothesis, the temperature used in the data analyses should be the atmospheric temperature of the region from which the bulk of water vapor of the precipitation originates. For instance, in the case of the equatorial oceanic region in 10°S–10°N, the temperature should be the air temperature over the equatorial oceanic region. Nevertheless, since we are dealing with large spatial and temporal (yearly) average values, the atmospheric temperature of the region tends to change proportionally with the corresponding SST and even the global surface temperature with a nearly unit ratio. For example, the ratio of temperature anomalies ( $\Delta T$ ) between the 30°S–30°N zone and the near-global zone (60°S–60°N) is 0.82, and 0.93 between the 10°S–10°N oceanic region and the near-global zone. Thus, for convenience, temperature of the 30°S–30°N zone can be used as the proxy. This is also consistent with the fact that the 30°S–30°N zone is the primary source of moisture for all regions discussed in this study. For further discussion on the use of near-global temperature rather than local or regional temperature, readers are referred to the work by Liu et al. (2009), which shows that, even for a small island like Taiwan, a near-global temperature gives better results than the local temperature.

The changes in precipitation intensity in all three latitude zones show a highly consistent general pattern, including a relatively large increase for the top 10% heavy precipitation, a rapid approach to zero near the fifth bin, and small decreases for light precipitation bins below the fifth bin. The consistency is remarkable, especially considering the fact that the 20°–45°N land area contains a large amount of gauge data from observations at meteorological stations while the 10°S–10°N oceanic region contains predominately satellite data, confirming the previous finding that the GPCP satellite data are consistent with observations of meteorological stations (Lau and Wu, 2007).

Changes in the industrialized 20°–45°N land area are generally more moderate compared to the clean equatorial oceans. This is expected according to the thermodynamic hypothesis because there is less extremely heavy precipitation at higher latitudes relative to the equatorial oceanic areas (Trenberth et al., 2003; Liu et al., 2009), but the opposite would have been expected if the aerosol effect is correct as there are more anthropogenic aerosols at higher latitudes in

the Northern Hemisphere.

The large increase of about 186%  $\text{K}^{-1}$  in the top 10% heavy precipitation in the 10°S–10°N oceanic region can have severe environmental impacts. Since the temperature of the 30°S–30°N zone has increased by about 0.68 in the last century, it scales to an increase of about 126% in the top 10% heavy precipitation of the 10°S–10°N oceanic region in that period. This can have a profound impact on the ecosystem of coastal areas in the equatorial region. Similar concerns should be raised for the 10°–20°N zone where tropical cyclones contribute to a major part of the top 10% heavy precipitation.

The consistency among the changes in precipitation intensity of all three latitude zones suggests that a common mechanism, i.e. global warming, is the primary cause of the changes in precipitation intensity. The increase of the top 10% precipitation being greater at lower latitude is consistent with previous findings (Liu et al., 2009; Shiu et al., 2012), and with global warming theory because there are stronger convective storms at lower latitudes than higher latitudes. On the other hand, one would expect a greater increase in precipitation intensity at higher latitudes if the effects of aerosols are the cause because there are more anthropogenic aerosols at higher latitudes than lower latitudes in the Northern Hemisphere. Therefore, it is reasonable to propose that the changes in precipitation intensity in all three latitude zones (1979–2007) are likely caused primarily by global warming rather than aerosol effects.

In regard to the total precipitation, by adding up the values of individual bins in Fig. 3, we find interesting significant trends of 28.6%  $\text{K}^{-1}$ , 2.3%  $\text{K}^{-1}$  and 1.7%  $\text{K}^{-1}$  for the equatorial 10°S–10°N oceanic region, 10°–20°N zone and 20°–45°N land zone, respectively. The relatively large increasing trend of the equatorial latitude zone is obviously related to the convergent ascending/wet zone of the Hadley cell, and the large trend appears to be a result of the wet-get-wetter mechanism (Mitchell et al., 1987; Held and Soden, 2006; Chou et al., 2013). Nevertheless, essentially all the increasing trends in the three latitude zones can be attributed to the increase in the top 30% heavy precipitation (i.e. heavy-get-heavier rather than wet-get-wetter), and the bottom 70% light and moderate precipitation bins show small and compensating changes. In other words, the increase in total precipitation in the equatorial region is the result of an enhancement in the heavy precipitation, which in turn is driven by global warming.

## 5. Changes of precipitation intensity in eastern China

Also plotted in Fig. 3 are changes in precipitation intensity derived from meteorological stations in eastern China. Given the substantial differences in geohydrological environments between eastern China and the 20°–45°N land area, as well as the coarse spatial and temporal resolution of GPCP data, the good agreement between the changes in precipitation intensities in the two areas is reassuring, particularly for

the top 10% heavy precipitation and the general pattern of increases in heavy precipitation and decreases in light precipitation. The agreement suggests that the change in precipitation intensity in eastern China is also likely caused primarily by global warming. Additional support for this notion can be seen in Figs. 4a–c, which depict annual average values of the total precipitation, bottom 10% light precipitation, and top 10% heavy precipitation, respectively, for the urban stations and the rural stations. As expected, the annual average total precipitation values show no significant trend (Fig. 4a). For the bottom 10% light precipitation, both the urban and rural values show significant decreasing trends and their linear rates of decrease are statistically identical (Fig. 4b). Fur-

thermore, the interannual variations are nearly identical between urban and rural stations, suggesting a common cause for these variations and trends rather than the difference in concentrations of aerosols between urban and rural stations. The changes in the top 10% heavy precipitation (Fig. 4c) also support this argument.

One could take exception to the above argument by claiming that rural stations in China are also highly polluted due to efficient dispersion and transport of air pollutants. To address this problem, we examine the precipitation data of Taiwan. During the summer, stations located in eastern Taiwan and small offshore islands tend to have clean background oceanic air with average  $PM_{10}$  concentrations of around  $20 \mu g m^{-3}$

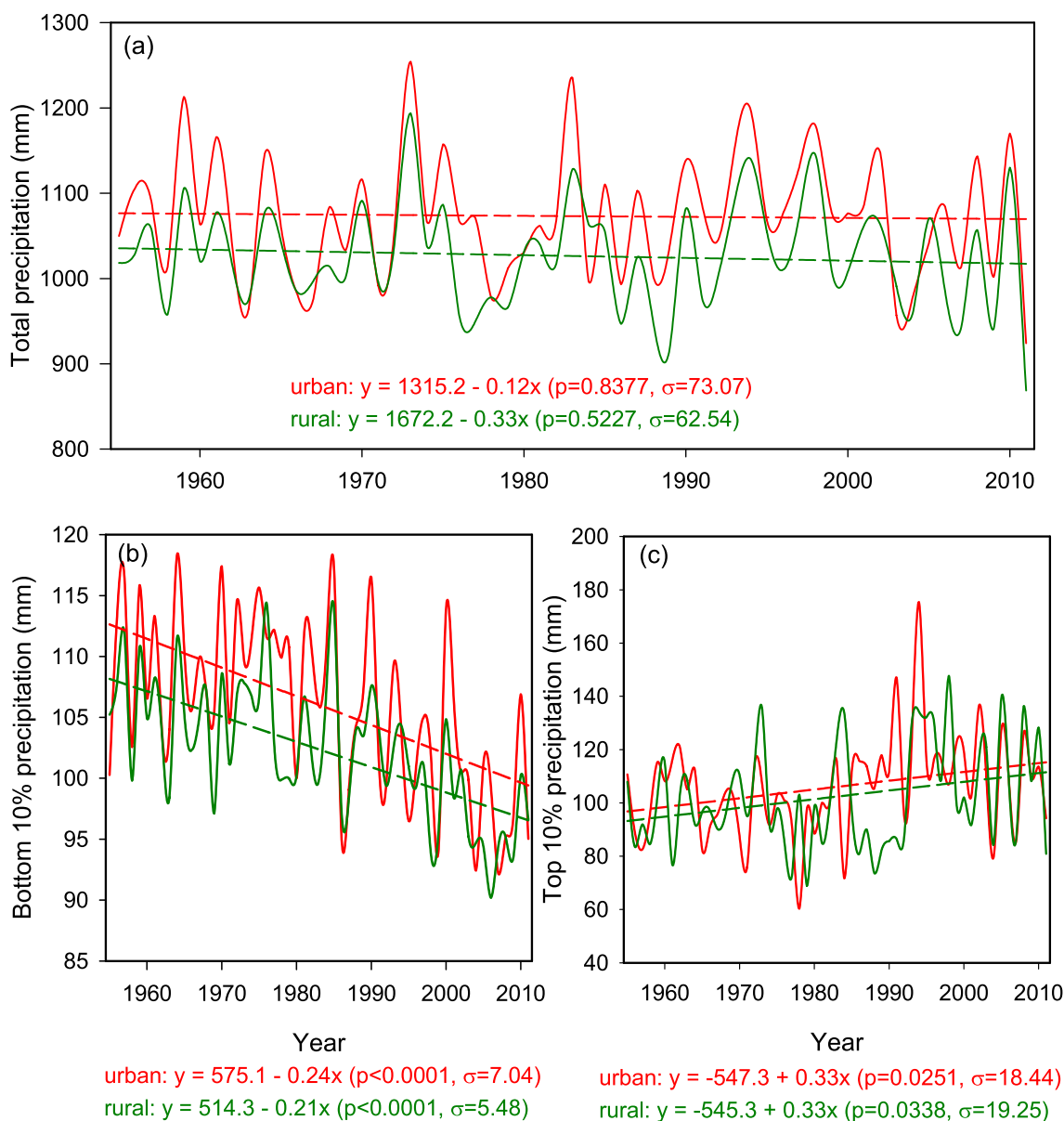


**Fig. 4.** Temporal variations of annual average amounts of precipitation (mm) with linear regression: (a) total precipitation; (b) bottom 10% light precipitation; (c) top 10% heavy precipitation. Red solid lines denote average values of 45 urban stations and green solid lines of 56 rural stations; red and green dashed lines are linear regressions for urban and rural stations, respectively. One standard deviation is denoted by  $\sigma$  (mm).

(mostly sea salt aerosols) (<http://taqm.epa.gov.tw/taqm/tw>) as the prevailing wind is southwesterly. In contrast, stations located in western Taiwan are polluted with average  $PM_{10}$  concentrations of around  $40 \mu\text{g m}^{-3}$ . In Fig. 5, we compare the temporal variations of 5-yr running average summer precipitation in polluted western Taiwan to that of clean eastern Taiwan and small offshore islands for the bottom 10% light precipitation and top 10% heavy precipitation. For the bottom 10% light precipitation, both the polluted region and clean region show significant decreasing trends (Fig. 5a). Similarly, both the polluted region and clean region show large increasing trends in the top 10% heavy precipitation (Fig. 5b). These results clearly imply that anthropogenic aerosols are not a major cause of the trends in light and heavy precipitation, while the thermodynamic theory offers a reasonable explanation for the trends.

We recognize that there may be a problem of the compensation effect with long temporal and large spatial averaging. For instance, the increase of heavy precipitation could occur in southern China in summer, but the decrease of light precipitation could occur in northern China in winter. We checked for this problem by performing three tests: first, by dividing eastern China into four sub-regions according to latitude from south to north; second, by examining individual stations in China and individual grids of GPCP data; and third, by examining monthly and seasonal precipitation for China and GPCP data. For low latitudes in GPCP data ( $30^{\circ}\text{S}$ – $30^{\circ}\text{N}$ ), analysis of monthly data renders results consistent with yearly data. Furthermore, the interannual difference method applied to individual grids of GPCP data in the low latitudes produces

statistically significant and consistent trends for the majority of bins of precipitation intensity. For China, all four sub-regions show decreases in the bottom 10% light precipitation, but the northernmost sub-region is not statistically significant. All four sub-regions show increases of the top 10% heavy precipitation, but none statistically significant. The statistics become worse for individual stations. Nevertheless, most of the stations show decreases of light precipitation, but the increases in heavy precipitation are more sporadic. Seasonal results also suffer from the problem of poor statistics. The results indicate that compensation is neither a common nor a serious problem, but rather that the sporadic nature of precipitation makes it difficult to derive significant signals when data from a very limited number of stations are used.

In conclusion, the increase in precipitation intensity with global warming is a widespread phenomenon of global scale, albeit with regional differences in magnitude and other characteristics. The increase in precipitation intensity derived from observations at the 101 stations in eastern China is consistent with global warming theory, not with the effects of anthropogenic aerosols.

Having drawn this conclusion, we acknowledge that, on a long-term basis, anthropogenic aerosols reduce global warming through their direct and indirect radiative effects (Solomon et al., 2007), and in turn affect the precipitation intensity. But this effect is to reduce precipitation intensity, opposite to the observed changes. We also note that our analysis is performed for annual time scales, the results of which may not be applicable to findings of episodic precipitation

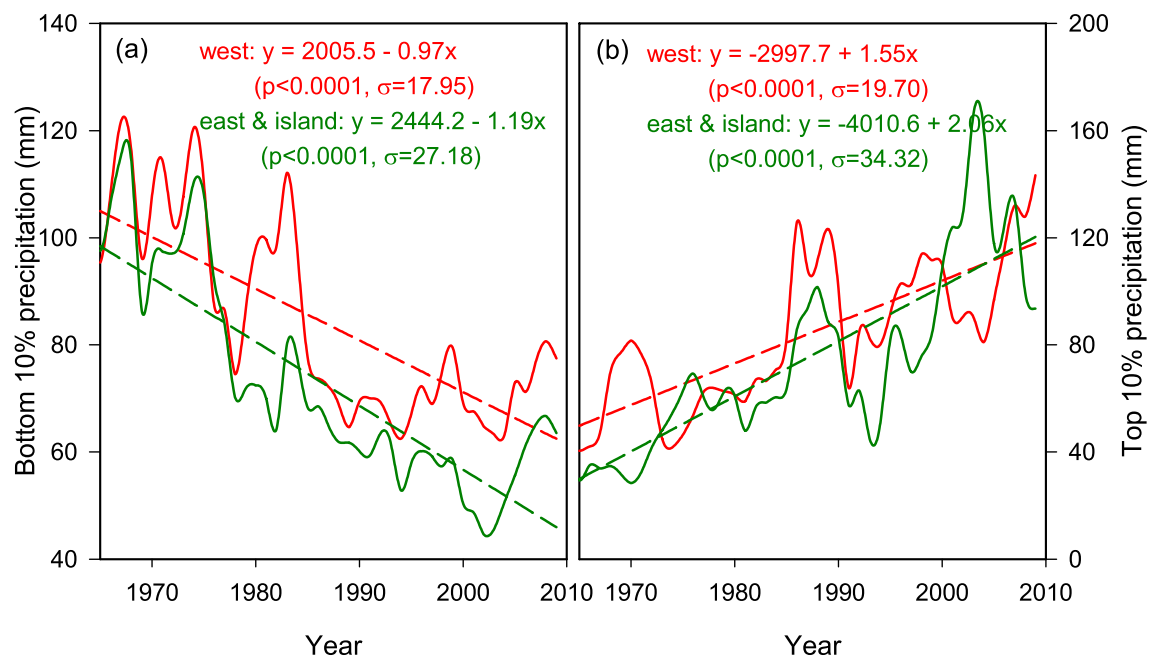


**Fig. 5.** Temporal variations of 5-yr running average amounts of summer precipitation (mm) with linear regression: (a) bottom 10% light precipitation; (b) top 10% heavy precipitation. Red solid lines denote average values of polluted stations located in western Taiwan and green solid lines of clean stations located in eastern Taiwan and offshore islands, respectively; red and green dashed lines are linear regressions for polluted and clean stations, respectively. One standard deviation is denoted by  $\sigma$  (mm).

studies. Finally, our result does not rule out anthropogenic aerosols as a secondary contributor to the observed increase in precipitation intensity.

## 6. Implications of increasing precipitation intensity

The implication of the causal relationship between global warming and the increase in precipitation intensity in widespread areas is profound. Increases in precipitation intensity and associated changes in the precipitation extremes can have severe impacts on the hydrological cycle and thus the entire ecosystem. It is clear that an increase in heavy precipitation increases the meteorological risk of floods and landslides. Light and moderate precipitation is a critical source of soil moisture as well as ground water. Decreases of light and moderate precipitation may increase the meteorological risk of droughts, particularly when coupled with increases in annual total dry days and consecutive dry days.

Figure 6 shows time series of observed annual total dry days, the occurrence of  $\geq 10$  consecutive dry days, days of the top 1% heavy precipitation, days of the top 10% heavy precipitation, and days of the bottom 10% light precipitation, for all 101 stations during the period 1955–2011. In addition, the annual occurrence of Palmer Drought Severity Index (PDSI)  $\leq -3$  in eastern China, which is an indicator for severe drought, is also plotted. All linear regressions passed the  $t$ -test at the  $p$ -value of 0.05. Remarkably, the annual days of the top 1% and 10% heavy precipitation increased by about 77% and 21% during the 57-year period, respectively. A more alarming increase was the annual total dry days, by about 28 days (13%) during this period, nearly a whole month. Moreover, the occurrence of  $\geq 10$  consecutive dry days increased even more in terms of percentage change (36%) than the total dry days. These increases in dry days and consecutive dry days significantly increase the meteorological risk of droughts. This is substantiated by the sharp increase (about 20 times) in the annual occurrence of PDSI  $\leq -3$  in eastern China during this period. This sharp increase in the annual occurrence of PDSI  $\leq -3$  is in good agreement with a previous study of this region (Dai et al., 2004). While these results have been seen in part in a number of previous studies (Ho et al., 2005; Liu et al., 2005; Zhai et al., 2005; Qian et al., 2007), the causal relationship between global warming and the increase in precipitation intensity established here implies that the substantial increased meteorological risk of floods and landslides in eastern China during the period 1955–2011 is was likely primarily due to global warming. Using the interannual difference method, we derive, for one degree Kelvin increase in the  $30^{\circ}\text{S}$ – $30^{\circ}\text{N}$  temperature, an increase of  $29.7\% \pm 15\%$  in the annual occurrence of  $\geq 10$  consecutive dry days, and a severe increase of  $221.6\% \pm 68.7\%$  in the annual occurrence of PDSI  $\leq -3$ .

There is good correlation/anti-correlation ( $R^2 > 0.55$ ) among the changes of annual days of the bottom 10% light precipitation, total dry days, the occurrence of  $\geq 10$

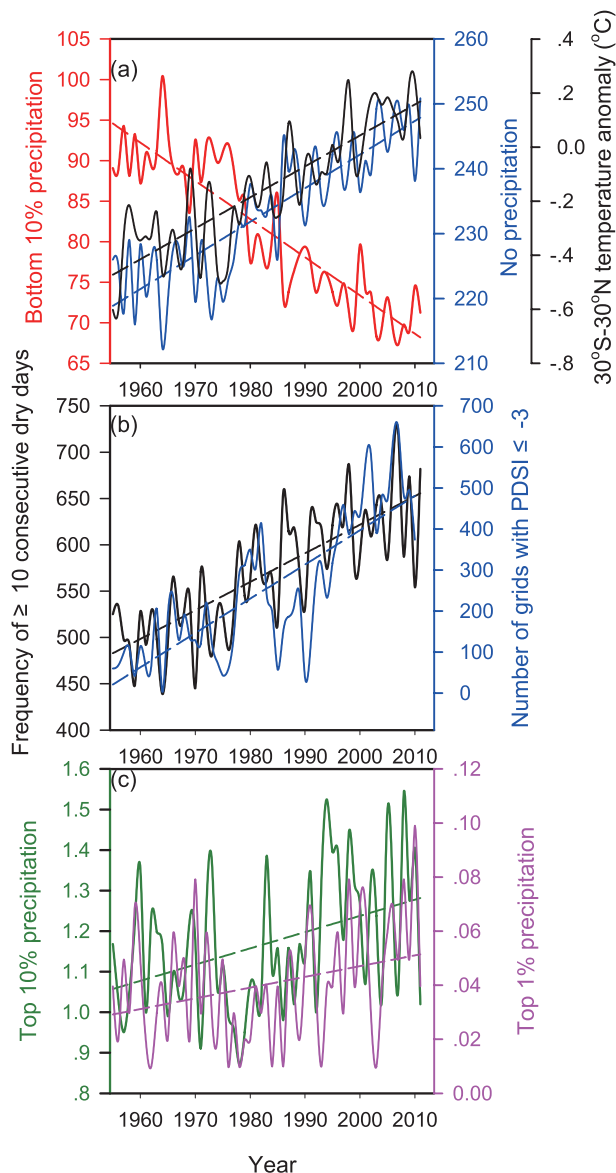


**Fig. 6.** Temporal variations of the annual average values of various precipitation parameters in eastern China. Solid lines denote annual average values; dashed lines are linear regressions. (a) Dry (no precipitation) days (blue, right coordinate), days of the bottom 10% light precipitation (red, left coordinate), and the  $30^{\circ}\text{S}$ – $30^{\circ}\text{N}$  temperature anomaly (black, right offset coordinate); (b) occurrence of 10 or more consecutive dry days (black, left coordinate) and number of grids with PDSI  $\leq -3$  (blue, right coordinate); (c) days of the top 1% heavy precipitation (purple, right coordinate) and days of the top 10% heavy precipitation (green, left coordinate).

consecutive dry days, and the occurrence of PDSI  $\leq -3$ , hinting a causal relationship among them. In particular, there is a remarkably high anti-correlation coefficient of  $-0.97$  between the dry days and bottom 10% light precipitation days. Moreover, the increase in dry days is about 90% compensated by the decrease in annual days of the bottom 10% light precipitation. The remainder is compensated by changes of the bottom 10%–40% light and moderate precipitation. These re-



sults can be logically understood as the category of dry days is theoretically the lightest category in the precipitation intensity spectrum, while the bottom 10% light precipitation is the second lightest category. Consequently, a shift in light precipitation toward heavy precipitation leaves more dry days.

As discussed at the beginning of the paper, significant increases of heavy precipitation and decreases of light precipitation have been reported over widespread areas within the 60°S–60°N latitudinal zone (Lau and Wu, 2007; Liu et al., 2009; Shiu et al., 2012; Lau et al., 2013). It follows that the substantial increases in the meteorological risk of droughts and floods due to global warming in eastern China in 1955–2011 found here are expected to occur in widespread areas within 60°S–60°N. Moreover, since increases of precipitation intensity with global warming are greater at lower latitudes (Liu et al., 2009), increases in the meteorological risk of droughts and floods are expected to be greater at lower latitudes.

## 7. Summary

We have presented observational evidence, theoretical arguments, and results from reanalysis (Shiu et al., 2012) and climate models (Sun et al., 2007) that support, in eastern China during the period 1955–2011, a causal link starting from global warming to an increase in precipitation intensity, to changes in precipitation extremes, and to greater meteorological risk of floods and droughts. Quantitatively, we find a severe increase of about 77% in annual days of the top 1% heavy precipitation, a decrease of about 20% in the annual amount of the bottom 10% light precipitation, an increase of 36% in the annual occurrence of  $\geq 10$  consecutive dry days, and an astonishing approximate 20-fold increase in the annual occurrence of  $\text{PDSI} \leq -3$  in eastern China during the period 1955–2011. Furthermore, these changes are expected to increase with greater future climate warming. More importantly, these changes are not limited to eastern China; similar changes have been observed in widespread regions, as cited in the introduction. Significant increases in the meteorological risk of droughts and floods are also expected to occur in these regions, and more severely at low latitudes (Liu et al., 2009), as a result of global warming. Adaptive actions such as flood and drought prevention, water resource management and land-use adjustment are imperative.

**Acknowledgements.** This work was supported in part by the Chinese Academy of Sciences Strategic Priority Research Program (Grant No. XDB05010500), the Clean Air Research Project in China (Grant No. 201509001), and the Sustainable Development Research Project of Academia Sinica, Consortium for Climate Change Study, funded by the National Science Council (Grant No. 100-2119-M-001-029-MY5). This work was sponsored by the Collaborative Innovation Center for Regional Environmental Quality and the State Key Joint Laboratory of Environmental Simulation and Pollution Control, Peking University. The ECMWF ERA-Interim data used in this study were obtained from the ECMWF data server.

We acknowledge the Global Precipitation Analysis, Laboratory for Atmospheres, NASA Goddard Space Flight Center (<http://precip.gsfc.nasa.gov/>), for providing the GPCP data, and the Climate and Global Dynamic's Climate Analysis Section, National Center for Atmospheric Research Earth System Laboratory (<http://www.cgd.ucar.edu/cas/catalog/climind/pdsi.html>), for providing the PDSI data. We also thank MAO You-Yu and WAN Chih-Wei for their assistance in the data analysis. We are grateful to the two anonymous reviewers for their useful reviews and advice, which led to an improved revised manuscript.

## REFERENCES

- Ackerman, A. S., and Coauthors, 1978: *Summary of METROMEX, Volume 2: Causes of Precipitation Anomalies*. Illinois State Water Survey, Urbana, Bulletin 63, 399 pp.
- Albrecht, B. A., 1989: Aerosols, cloud microphysics, and fractional cloudiness. *Science*, **245**, 1227–1230, doi: 10.1126/science.245.4923.1227.
- Allen, M. R., and W. J. Ingram, 2002: Constraints on future changes in climate and the hydrologic cycle. *Nature*, **419**, 224–232, doi: 10.1038/nature01092.
- Andreae, M. O., D. Rosenfeld, P. Artaxo, A. A. Costa, G. P. Frank, K. M. Longo, and M. A. Silva-Dias, 2004: Smoking rain clouds over the Amazon. *Science*, **303**, 1337–1342, doi: 10.1126/science.1092779.
- Benestad, R. E., 2013: Association between trends in daily rainfall percentiles and the global mean temperature. *J. Geophys. Res.*, **118**, 10 802–10 810, doi: 10.1002/jgrd.50814.
- Boucher, O., and Coauthors, 2013: Clouds and Aerosols. *Climate Change 2013: The Physical Science Basis. Contribution of Working Group I to the Fifth Assessment Report of the Intergovernmental Panel on Climate Change.*, T. F. Stocker, and Coauthors, Eds., Cambridge Univ. Press, Ch. 7, 571–685.
- Chou, C., J. C. H. Chiang, C.-W. Lan, C.-H. Chung, Y.-C. Liao, and C.-J. Lee, 2013: Increase in the range between wet and dry season precipitation. *Nature Geoscience*, **6**, 263–267, doi: 10.1038/ngeo1744.
- Cubasch, U., and Coauthors, 2001: Projections of Future Climate Change. *Climate Change 2001: The Scientific Basis.*, J. T. Houghton and Y. H. Ding, Eds., Cambridge Univ. Press, Ch. 9, 524–582.
- Dai, A., P. J. Lamb, K. E. Trenberth, M. Hulme, P. D. Jones, and P. P. Xie, 2004: The recent Sahel drought is real. *Inter. J. Climatol.*, **24**, 1323–1331, doi: 10.1002/joc.1083.
- Dai, J., Y. Xing, D. Rosenfeld, and X. H. Xu, 2008: The suppression of aerosols to the orographic precipitation in the Qinling Mountains. *Chinese J. Atmos. Sci.*, **32**, 1319–1332 (in Chinese).
- Fujibe, F., N. Yamazaki, M. Katsuyama, and K. Kobayashi, 2005: The increasing trend of intense precipitation in Japan based on four-hourly data for a hundred years. *Sola*, **1**, 41–44, doi: 10.2151/sola.2005.012.
- Gong, D.-Y., C.-H. Ho, D. L. Chen, Y. Qian, Y.-S. Choi, and J. Kim, 2007: Weekly cycle of aerosol-meteorology interaction over China. *J. Geophys. Res.*, **112**, D22202, doi: 10.1029/2007jd008888.
- Goswami, B. N., V. Venugopal, D. Sengupta, M. S. Madhusoodanan, and P. K. Xavier, 2006: Increasing trend of extreme rain events over India in a warming environment. *Sci-*

- ence, **314**, 1442–1445, doi: 10.1126/science.1132027.
- Groisman, P. Y., R. W. Knight, D. R. Easterling, T. R. Karl, G. C. Hegerl, and V. N. Razuvayev, 2005: Trends in intense precipitation in the climate record. *J. Climate*, **18**, 1326–1350, doi: 10.1175/jcli3339.1.
- Hansen, J., M. Sato, and R. Ruedy, 1997: Radiative forcing and climate response. *J. Geophys. Res.*, **102**, 6831–6864, doi: 10.1029/96jd03436.
- Held, I. M., and B. J. Soden, 2006: Robust responses of the hydrological cycle to global warming. *J. Climate*, **19**, 5686–5699, doi: 10.1175/jcli3990.1.
- Ho, C.-H., J.-H. Kim, W. K. M. Lau, K.-M. Kim, D. Gong, and Y.-B. Lee, 2005: Interdecadal changes in heavy rainfall in China during the northern summer. *The Journal of Terrestrial, Atmospheric and Oceanic Sciences*, **16**, 1163–1176.
- Jiang, J. H., H. Su, M. R. Schoeberl, S. T. Massie, P. Colarco, S. Platnick, and N. J. Livesey, 2008: Clean and polluted clouds: Relationships among pollution, ice cloud, and precipitation in South America. *Geophys. Res. Lett.*, **35**, L10804, doi: 10.1029/2010gl043792.
- Jiang, Z. H., Y. C. Shen, T. T. Ma, P. M. Zhai, and S. D. Fang, 2014: Changes of precipitation intensity spectra in different regions of mainland China during 1961–2006. *Journal of Meteorological Research*, **28**, 1085–1098.
- Jones, P. D., and A. Moberg, 2003: Hemispheric and large-scale surface air temperature variations: An extensive revision and an update to 2001. *J. Climate*, **16**, 206–223, doi: 10.1175/1520-0442(2003)016<0206:HALSSA>2.0.CO;2.
- Karl, T. R., and R. W. Knight, 1998: Secular trends of precipitation amount, frequency, and intensity in the United States. *Bull. Amer. Meteorol. Soc.*, **79**, 231–241, doi: 10.1175/1520-0477(1998)079<0231:Stopaf>2.0.Co;2.
- Klein Tank, A. M. G., and G. P. Können, 2003: Trends in indices of daily temperature and precipitation extremes in Europe, 1946–99. *J. Climate*, **16**, 3665–3680, doi: 10.1175/1520-0442(2003)016<3665:TIIOdT>2.0.CO;2.
- Koren, I., J. V. Martins, L. A. Remer, and H. Afargan, 2008: Smoke invigoration versus inhibition of clouds over the Amazon. *Science*, **321**, 946–949, doi: 10.1126/science.1159185.
- Lau, K.-M., and H.-T. Wu, 2007: Detecting trends in tropical rainfall characteristics, 1979–2003. *Int. J. Climatol.*, **27**, 979–988, doi: 10.1002/joc.1454.
- Lau, K.-M., and H.-T. Wu, 2011: Climatology and changes in tropical oceanic rainfall characteristics inferred from tropical rainfall measuring mission (TRMM) data (1998–2009). *J. Geophys. Res.*, **116**, D17111, doi: 10.1029/2011jd015827.
- Lau, W. K.-M., H.-T. Wu, and K.-M. Kim, 2013: A canonical response of precipitation characteristics to global warming from CMIP5 models. *Geophys. Res. Lett.*, **40**, 3163–3169, doi: 10.1002/grl.50420.
- Levin, Z., and W. R. Cotton, 2009: *Aerosol Pollution Impact on Precipitation: A Scientific Review*. Springer Verlag, 386 pp.
- Lin, J. C., T. Matsui, R. A. Pielke, and C. Kummerow, 2006: Effects of biomass-burning-derived aerosols on precipitation and clouds in the Amazon Basin: a satellite-based empirical study. *J. Geophys. Res.*, **111**, D19204, doi: 10.1029/2005jd006884.
- Liu, B. H., M. Xu, M. Henderson, and Y. Qi, 2005: Observed trends of precipitation amount, frequency, and intensity in China, 1960–2000. *J. Geophys. Res.*, **110**, D08103, doi: 10.1029/2004jd004864.
- Liu, S. C., C. B. Fu, C.-J. Shiu, J.-P. Chen, and F. T. Wu, 2009: Temperature dependence of global precipitation extremes. *Geophys. Res. Lett.*, **36**, L17702, doi: 10.1029/2009gl040218.
- Lu, Z., and Coauthors, 2010: Sulfur dioxide emissions in China and sulfur trends in East Asia since 2000. *Atmos. Chem. Phys.*, **10**, 6311–6331, doi: 10.5194/acp-10-6311-2010.
- Manton, M. J., and Coauthors, 2001: Trends in extreme daily rainfall and temperature in Southeast Asia and the South Pacific: 1961–1998. *Int. J. Climatol.*, **21**, 269–284, doi: 10.1002/joc.610.
- Mitchell, J. F. B., C. A. Wilson, and W. M. Cunningham, 1987: On CO<sub>2</sub> climate sensitivity and model dependence of results. *Quart. J. Roy. Meteor. Soc.*, **113**, 293–322, doi: 10.1256/sm-sqj.47516.
- Mitchell, T. D., and P. D. Jones, 2005: An improved method of constructing a database of monthly climate observations and associated high-resolution grids. *Int. J. Climatol.*, **25**, 693–712, doi: 10.1002/joc.1181.
- National Bureau of Statistics of China, 2012: *China Statistical Yearbook 2012*. China Statistics Press, Beijing, 1069 pp. (in Chinese)
- National Research Council, 2003: *Critical Issues in Weather Modification Research*. The National Academies Press, Washington, D. C., USA, 143 pp.
- Peterson, T. C., and R. S. Vose, 1997: An overview of the global historical climatology network temperature database. *Bull. Amer. Meteor. Soc.*, **78**, 2837–2849, doi: 10.1175/1520-0477(1997)078<2837:A00TGH>2.0.CO;2.
- Qian, W. H., J. K. Fu, and Z. W. Yan, 2007: Decrease of light rain events in summer associated with a warming environment in China during 1961–2005. *Geophys. Res. Lett.*, **34**, L11705, doi: 10.1029/2007gl029631.
- Qian, Y., D. Y. Gong, and R. Leung, 2010: Light rain events change over North America, Europe, and Asia for 1973–2009. *Atmospheric Science Letters*, **11**, 301–306, doi: 10.1002/asl.298.
- Ramanathan, V., P. J. Crutzen, J. T. Kiehl, and D. Rosenfeld, 2001: Aerosols, climate, and the hydrological cycle. *Science*, **294**, 2119–2124, doi: 10.1126/science.1064034.
- Rosenfeld, D., and Coauthors, 2008: Flood or drought: How do aerosols affect precipitation? *Science*, **321**, 1309–1313, doi: 10.1126/science.1160606.
- Semenov, V. A., and L. Bengtsson, 2002: Secular trends in daily precipitation characteristics: greenhouse gas simulation with a coupled AOGCM. *Climate Dyn.*, **19**, 123–140, doi: 10.1007/s00382-001-0218-4.
- Shiu, C.-J., S. C. Liu, C. B. Fu, A. Dai, and Y. Sun, 2012: How much do precipitation extremes change in a warming climate? *Geophys. Res. Lett.*, **39**, L17707, doi: 10.1029/2012gl052762.
- Smith, T. M., R. W. Reynolds, T. C. Peterson, and J. Lawrimore, 2008: Improvements to NOAA’s historical merged land ocean surface temperature analysis (1880–2006). *J. Climate*, **21**, 2283–2296, doi: 10.1175/2007jcli2100.1.
- Solomon, S., and Coauthors, 2007: *Climate Change 2007: The Physical Scientific Basis. Contribution of Work Group I to the Fourth Assessment Report of the Intergovernmental Panel on Climate Change*. Cambridge Univ. Press, 996 pp.
- Streets, D. G., N. Y. Tsai, H. Akimoto, and K. Oka, 2000: Sulfur dioxide emissions in Asia in the period 1985–1997. *Atmos. Environ.*, **34**, 4413–4424, doi: 10.1016/S1352-2310(00)00187-4.
- Sun, Y., S. Solomon, A. Dai, and R. W. Portmann, 2007: How

- often will it rain? *J. Climate*, **20**, 4801–4818, doi: 10.1175/jcli4263.1.
- Tao, W.-K., J.-P. Chen, Z. Q. Li, C. E. Wang, and C. D. Zhang, 2012: Impact of aerosols on convective clouds and precipitation. *Rev. Geophys.*, **50**, doi: 10.1029/2011rg000369.
- Trenberth, K. E., 1998: Atmospheric moisture residence times and cycling: Implications for rainfall rates and climate change. *Climatic Change*, **39**, 667–694, doi: 10.1023/A:1005319109110.
- Trenberth, K. E., A. Dai, R. M. Rasmussen, and D. B. Parsons, 2003: The changing character of precipitation. *Bull. Amer. Meteor. Soc.*, **84**, 1205–1217, doi: 10.1175/bams-84-9-1205.
- Trenberth, K. E., and Coauthors, 2007: Observations: Surface and Atmospheric Climate Change. *Climate Change 2007: The Physical Science Basis. Contribution of Working Group I to the Fourth Assessment Report of the Intergovernmental Panel on Climate Change*, S. Solomon, and Coauthors, Eds., Cambridge University Press, Ch. **9**, 747–845.
- Vose, R. S., R. L. Schmoyer, P. M. Steurer, T. Peterson, R. Heim, T. Karl, and J. Eischeid, 1992: *The Global Historical Climatology Network: Long-Term Monthly Temperature, Precipitation, Sea Level Pressure, and Station Pressure Data*. Carbon Dioxide Information Analysis Center, Oak Ridge National Laboratory, Oak Ridge, TN., 325 pp, doi: 10.3334/CDIAC/cli.ndp041.
- Wang, F., and Q. S. Ge, 2012: Estimation of urbanization bias in observed surface temperature change in China from 1980 to 2009 using satellite land-use data. *Chinese Science Bulletin*, **57**, 1708–1715.
- Wang, X. L., and P. M. Zhai, 2008: Changes in China's precipitation in various categories during 1957–2004. *Journal of Tropical Meteorology*, **24**, 459–466.
- Warner, J., 1971: Smoke from sugar-cane fires and rainfall. *Conference on Weather Modification*, Canberra, ACT., Amer. Meteor. Soc., 191–192.
- Warner, J., and S. Twomey, 1967: The production of cloud nuclei by cane fires and the effect on cloud droplet concentration. *J. Atmos. Sci.*, **24**, 704–706, doi: 10.1175/1520-0469(1967)024<0704:Tpocnb>2.0.Co;2.
- Wu, F. T., and C. B. Fu, 2013: Change of precipitation intensity spectra at different spatial scales under warming conditions. *Chinese Science Bulletin*, **58**, 1385–1394.
- Xie, P. P., and Coauthors, 2003: GPCP Pentad precipitation analyses: An experimental dataset based on gauge observations and satellite estimates. *J. Climate*, **16**, 2197–2214, doi: 10.1175/2769.1.
- Xue, Y., T. M. Smith, and R. W. Reynolds, 2003: Interdecadal changes of 30-yr SST normals during 1871–2000. *J. Climate*, **16**, 1601–1612, doi: 10.1175/1520-0442-16.10.1601.
- Yang, H. L., H. Xiao, and Y. C. Hong, 2011a: Progress in impacts of aerosol on cloud properties and precipitation. *Climatic and Environmental Research*, **16**, 525–542. (in Chinese)
- Yang, X. C., Y. L. Hou, and B. D. Chen, 2011b: Observed surface warming induced by urbanization in east China. *J. Geophys. Res.*, **116**, D14113, doi: 10.1029/2010jd015452.
- Zhai, P. M., X. B. Zhang, H. Wan, and X. H. Pan, 2005: Trends in total precipitation and frequency of daily precipitation extremes over China. *J. Climate*, **18**, 1096–1108, doi: 10.1175/jcli-3318.1.
- Zhu, J., Y. C. Zhang, and D. Q. Huang, 2009: Analysis of changes in different-class precipitation over eastern China under global warming. *Plateau Meteorology*, **28**, 889–896. (in Chinese)